

## The wake behind the sphere; analysis of vortices during transition from steadiness to unsteadiness<sup>\*)</sup>

W. PRZĄDKA<sup>1)</sup>, J. MIEDZIK<sup>1)</sup>, K. GUMOWSKI<sup>1)</sup>,  
S. GOUJON-DURAND<sup>2)</sup>, J. E. WESFREID<sup>2)</sup>

<sup>1)</sup> *Warsaw University of Technology  
Institute of Aeronautics and Applied Mechanics  
ul. Nowowiejska 24, 00-665 Warsaw, Poland*

<sup>2)</sup> *PMMH – ESPCI, CNRS 7636  
10 rue Vauquelin, 75231 Paris Cedex 05, France*

THIS PAPER REPORTS about an experimental investigation of the wake behind a solid sphere on a low velocity hydrodynamical channel for the Reynolds number in the range 250–310. The aim of the work is to analyze the size and shape of the vortices' cores and its change as a function of the Reynolds number. Special attention is paid to the transition from stationary flow, characterized by two counter-rotating longitudinal vortices, to instationary flow. The two-coloured visualization of the wake in steady and unsteady regimes is also presented.

### 1. Introduction

THE SPHERE POSES an example of the simplest axisymmetric body. A large number of experimental and numerical studies of the wake behind the sphere has been performed. The wake is characterized by three different flow regimes. Previous visualizations carried out by TANEDA [1], MAGARVEY and BISHOP [2] revealed that the separation from the rear of the sphere occurs at the Reynolds number ( $Re = Ud/\nu$ ) about 20. Up to  $Re = 212$  the wake has an axisymmetric stationary ring structure and a recirculation region grows as  $Re$  increases. With the  $Re \simeq 212$  the wake splits, with the axisymmetry breaking, into two parallel counter-rotating vortices. The flow axisymmetry is replaced by a plane symmetry. This double-thread wake was observed to remain steady. The second transition occurs with  $Re \simeq 265$  and the wake becomes eventually unsteady, with peculiar periodic loops shedding as so-called hairpin vortices, preserving the plane symmetry. It is notable that a majority of experimental visualizations (e.g. ACHENBACH [3], ORMIÈRES [4]) show that hairpin vortices are all shed with the same orientation. For Reynolds number higher than 350 the shed-

---

<sup>\*)</sup>The paper was presented at XVIII Polish Conference of Fluid Mechanics (KKMP), Jastrzębia Góra, 21–25 September, 2008.

ding changes its character and two small hairpins following one big hairpin are observed. For  $Re > 500$  the flow becomes turbulent. These observations are in accordance with numerical simulations such as TOMBOULIDES *et al.* [5] and JOHNSON & PATEL [6].

Recent literature is mainly focused on second transition from steady to unsteady wake, particularly to the mechanism of hairpin vortex forming and shedding. Despite all the efforts, this phenomenon is still not fully described and many different theories around the hairpins shedding have been published. The numerical and experimental investigations, concerning hairpin shedding and forming, are in contradiction with each other. Particularly the double-hairpin theory, observed in the numerical results, has never been confirmed in the experiments. With reference to the still open problem of the transition to non-stationarity regime and to hairpins forming, the new experimental investigations were performed. The aim of the present study is to understand this phenomenon better, by obtaining experimentally the size and shape of the vortices' cores and its interactions as a function of the Reynolds number, in the state around the second bifurcation, what has never been experimentally determined ([7, 8]). In addition, two-coloured visualization of the second and third regime has been presented.

## 2. Experimental details

All measurements of the wake behind the sphere (diameter  $d = 16$  mm) were carried out in a horizontal water channel with a square section ( $100 \times 100$  mm<sup>2</sup>) and length equal to 860 mm, which is longer than 50 sphere diameters. The sphere was fixed on a rigid upstream bent pipe. The pipe was inclined with free stream of an angle of  $3^\circ$  (Fig. 1) The support's influence on perturbations on the flow is negligible, but determines the orientation of the symmetry plane. Typical velocities  $U$  were 4–40 mm/s and were deduced from flow mass rate measurement. The velocity was controlled by means of throttling valves. Water temperature was measured during the experiment by a high-precision mercury thermometer with an uncertainty of  $\pm 0.1^\circ$ .

This set-up allows to precise the increment in the Reynolds number value by  $1 \pm 0.5$ . The wake visualization was performed by means of argon laser

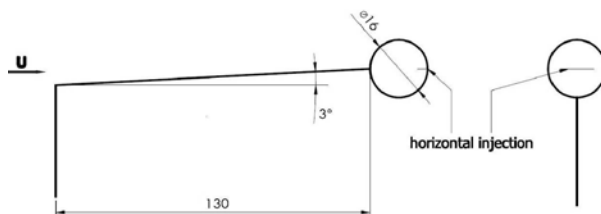


FIG. 1. Scheme of the holding of the sphere, including dye injection principle.

(50 mW) using Laser Induced Fluorescence (LIF) and diluted ink dye. In the first case, fluorescence dye was fed through the support pipe and horizontal slit in the sphere into recirculation zone. In the second case – dye in two different colours was injected into the upstream flow through two thin tubes. For both instances no difference in the recirculation bubble was found, what indicates that dye injection has no influence on the return flow. All the experimental measurements were done with the Particle Image Velocimetry (PIV) optical method using titanium dioxide ( $\text{TiO}_2$ ) particles. PIV image acquisition and post-processing were conducted using LaVision DaVis software which synchronized ImagePro  $1600 \times 1200$  12-bit CCD camera (with Nikon f35 mm, f50 mm and f105 mm lenses recording double-frame pairs of images at maximum 15 Hz) with two rod Nd:YAG pulsed laser (15 mJ). Image pairs were taken with the frequency of 10 Hz and the time spacing between images in pair was set to  $33340 \mu\text{s}$ . For each Reynolds number 300 image pairs were used for statistics. Vector calculations were computed using cross-correlation method and multi-pass iteration (window decreasing size:  $128 \times 128$  to  $16 \times 16$  with 25% overlap and 2 passes). PIV images were taken in the plane perpendicular to the flow stream. The measurements were limited to two planes: 2.5 and 5 diameters, downstream from the center of the sphere. The length of the recirculation zone in the considered Reynolds number range reaches about 1.5 diameters.

### 3. Results

Experimental investigations were performed at the Reynolds numbers between 250 and 310, which covers the transition to periodic state. As recalled in the Introduction, before second bifurcation a steady pair of opposite-sign stream-wise vortices is observed in the wake. The visualization (Fig. 2a) of the stationary non-axisymmetric wake shows the analogy with this statement. Increasing the Reynolds number over the value of 275 results in revealing the connected dye

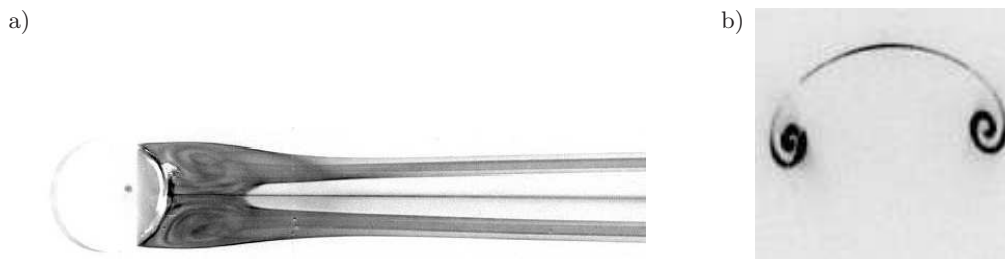


FIG. 2. Two steady counter rotating vortices – top (a) and back (b) view for  $\text{Re} 250$ .



FIG. 3. Visualization of the periodic vortex shedding for  $Re = 300$  (side view).

loops with respect to the planar symmetry, as shown in the Fig. 3, what also corresponds to previous numerical and experimental results.

The flow visualization can give the impression that the vortex has circular shape and is relatively small compared to the sphere diameter (Fig. 2b). The PIV results do not confirm these observations. As it can be seen in the Fig. 4a, the vortex has an elliptical shape with a longer diameter oriented vertically, what is in a good accordance with the physics of vortex. Streamwise vorticity contours, which are shown in the Fig. 4b, reveal a very interesting fact – the maximum vorticity does not lie in the geometrical center of the vortex, but is directed towards the plane of the symmetry. This observation proves the existence of very strong interactions between vortices. The shift of the vorticity centers was also observed in the numerical investigation performed by THOMPSON *et al.* [9]. To measure the size of the vortex in a function of the Reynolds number, the vorticity fields generated through LaVision DaVis software from PIV images taken in a plane perpendicular to the streamwise flow were used. Due to the noise existence, the vorticity peaks were observed in the flow regions where they were not expected. These noise of the vorticity were analyzed and tabled, for different Reynolds numbers. The highest value of the vorticity observed in the region, where vortex-free flow was expected, was assumed to pose the noise limit and its value is equal to  $0.5 \text{ 1/s}$ . It is supposed that the vortex

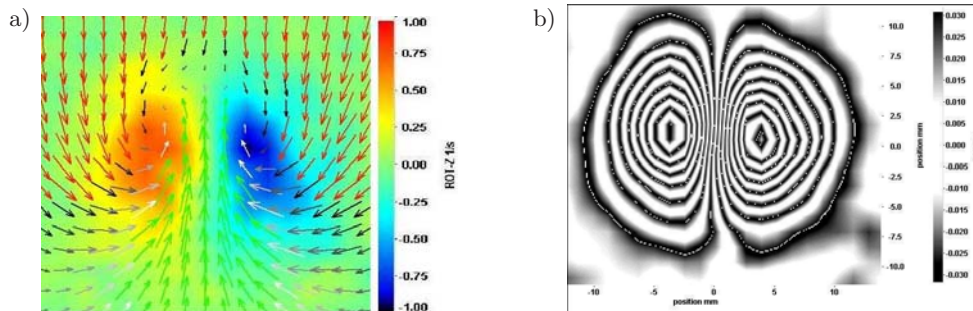


FIG. 4. a) Streamwise vorticity field in 2.5 diameters downstream from the center of the sphere for  $Re = 260$ , b) Streamwise vorticity contours in 2.5 diameters downstream from the center of the sphere for  $Re = 260$ .

exists in the area where the vorticity is higher than the noise level. The vorticity on the horizontal line crossing the maximum of vorticity were plotted (Fig. 5). On the basis of the plot it was possible to obtain horizontal diameter  $a_z$ , which is the width of the range of the vorticity higher than the noise limit. Vertical diameter  $a_y$  was measured analogically. For the Reynolds numbers higher than critical, when unsteady wake occurs and the flow is fully three-dimensional, vorticity fields are time-dependent, because the angle between vortices and the laser sheet changes in time. In this case the whole vorticity fields in a period were analyzed. The highest vorticity was observed in the image, which corresponds to the perpendicularity between vortices and the laser sheet. This image with the highest vorticity was the base for obtaining its horizontal and vertical diameters.

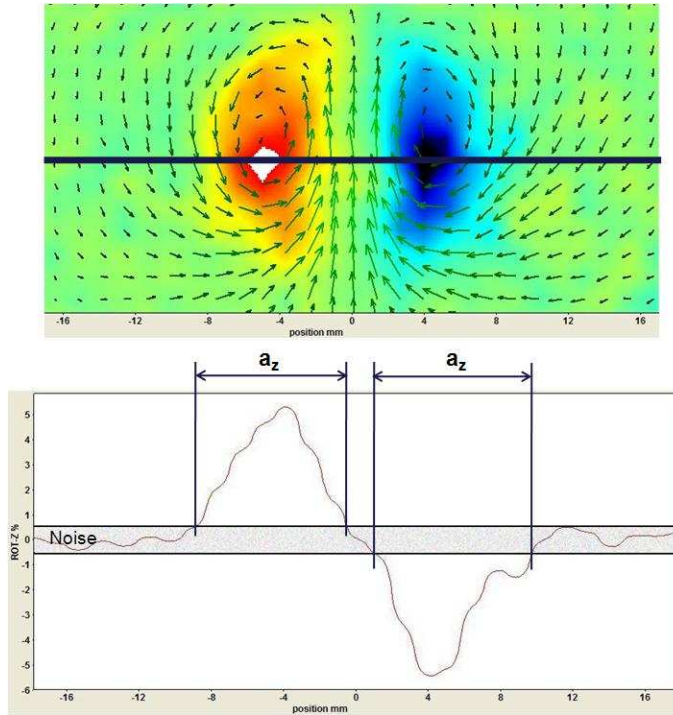


FIG. 5. Streamwise vorticity plotted on the horizontal line crossing the maximum vorticity.

In Fig. 6 the horizontal and vertical vortex dimensions relatively to the sphere diameter are presented. In the position corresponding to 2.5 diameters downstream from the sphere center, which is very near to the recirculation area, the core seems to preserve its size. In the distance equal to 5 diameters downstream from the center of the sphere, the dimensions decrease slowly and, approaching

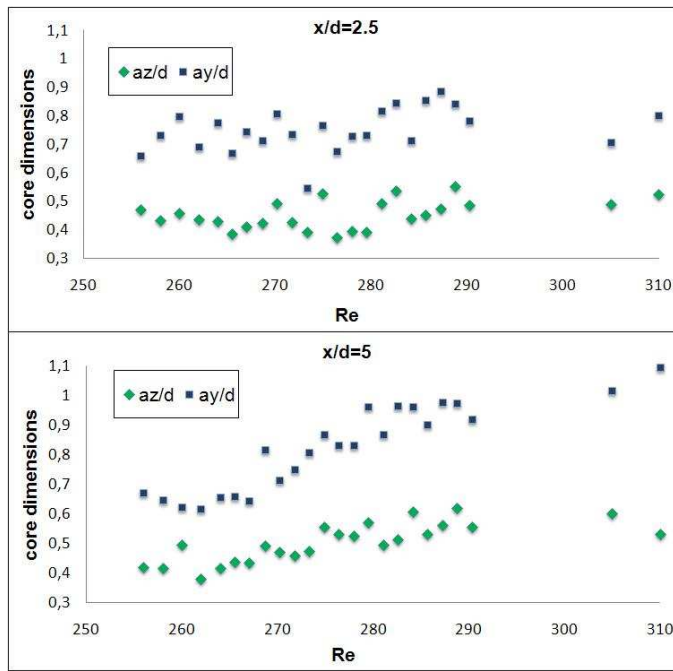


FIG. 6. Core dimensions in 2 different positions: 2.5 and 5 diameters downstream from the center of the sphere.

the critical Reynolds number, rapid, linear growth of vortices' dimensions can be noticed. As shown in the Fig. 7, vortices' cores are much greater than it can be seen on the visualization patterns.

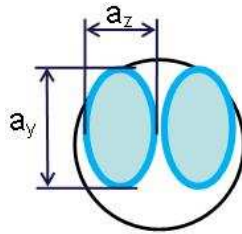


FIG. 7. The proportion of vortices' cores dimensions to sphere diameter for  $Re = 260$ .

The ratio of vertical to horizontal dimension was also calculated. According to the Fig. 8 it can be postulated that both dimensions ascend proportionally with the Reynolds number, even during the steady-unsteady bifurcation.

By means of classical visualization with two different colours it was found that fluid in the recirculation zone and in the far wake, does not cross the planar

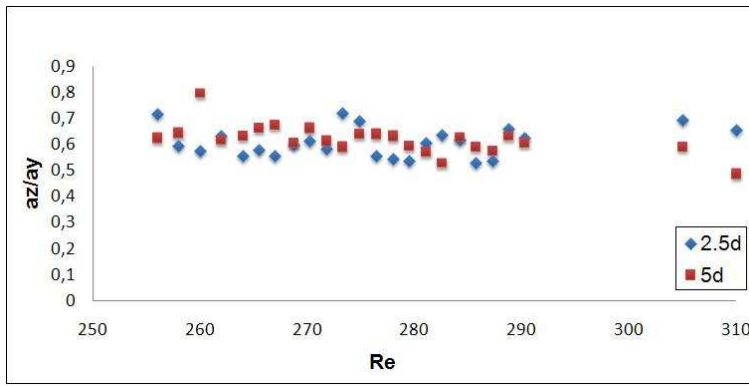


FIG. 8. The ratio of horizontal to vertical vortex core dimension as a function of the Reynolds number.

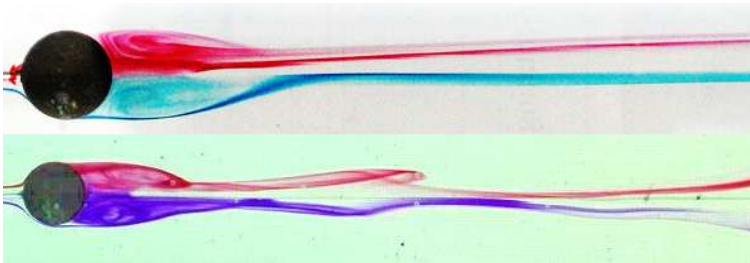


FIG. 9. Visualization with two different colours of steady and unsteady wake. Dye is fed to the flow 10 diameters upstream from the center of the sphere.

symmetry (Fig. 9). The existence of only one pathline, which joins the two regions of the recirculation zone determined by the symmetry plane, has been found. This was observed for the second and third regime. The visualization shows also that small oscillations of the vortices in a wake can be seen prior to the second threshold (Fig. 10). It has been noticed that these oscillations grow with the Reynolds number. This phenomenon is described in details by MIEDZIK *et al.* [10].

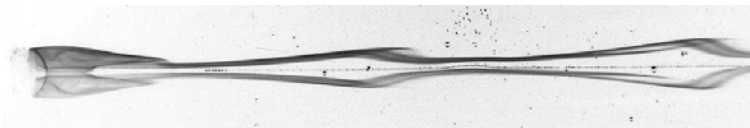


FIG. 10. Visualization of the wake for the Reynolds number prior to the second transition.

#### 4. Conclusions

This paper has examined sizes and shapes of the vortices' cores around the second transition of non-stationary flow regime. It was found that vortices are elliptical and relatively great compared to the sphere diameter. The vortices grow proportionally with the Reynolds number and this dependence is not disturbed by second bifurcation. It was also stated that the vortex streamwise vorticity is strongly asymmetrical and the maximum vorticity value is directed towards the planar symmetry.

#### References

1. J. TANEDA, *Experimental investigation of the wake behind a sphere at low Reynolds number*, J. Phys. Soc. Jpn., **11**, 1104–1108, 1956.
2. R. MAGARVEY, R.L. BISHOP, *Transition ranges for three-dimensional wakes*, Can. J. Phys., **39**, 1418–1422, 1961.
3. E. ACHENBACH, *Vortex shedding from spheres*, J. Fluid Mech., **62**, 209–221, 1974.
4. D. ORMIÈRES, *Etude expérimentale et modélisation du sillage d'une sphère à bas nombre de Reynolds*, PhD thesis, Université de Provence, France, 1999.
5. S. ORSZAG, A.G. TOMBOULIDES, G.E. KARNIADAKIS, *Direct and large eddy simulations of axisymmetric wakes*, AIAA Paper, p. 546, 1993.
6. T.A. JOHNSON, V.C. PATEL, *Flow past a sphere up to a Reynolds number of 300*, J. Fluid Mech., **378**, 19–70, 1999.
7. D. ORMIÈRES, M. PROVANSAL, *Transition to turbulence in the wake of a sphere*, Physical Review Letters, **83**, 80–83, 1999.
8. L. SCHOUVEILER AND M. PROVANSAL, *Self-sustained oscillations in the wake of a sphere*, Physics of Fluids, **14**, 3846–3854, 2001.
9. M.C. THOMPSON, T. LEWEKE, M. PROVANSAL, *Kinematics and dynamics of sphere wake transition*, J. Fluids Struct., **15**, 575–585, 2002.
10. K. GUMOWSKI, J. MIEDZIK, S. GOUJON-DURAND, P. JENFFER, J.E. WESFREID, *Transition to a time-dependent state of fluid flow in the wake of a sphere*, Phys. Rev. E, **77**, 5:055308, 2008.

Received May 29, 2008; revised version November 13, 2008.

---